Engineering Symposium at Bánki
(ESB 2024)

Seismic analysis of tunnel-form reinforced concrete structures subjected to low-intensity earthquake actions

[1]Kamaran Mohammed Kareem, [2]Bakhtyar Saleh Ahmmad

[1] *University of Halabja, Department of Civil Engineering, Halabja, Iraq*
kamaran.kareem@uoh.edu.iq
[2] *Obuda University, Doctoral School of Safety and Security Sciences, Budapest, Hungary,*
bakhtyar.ahmman@phd.uni-obuda.hu

Abstract

Multi-story reinforced concrete tunnel form buildings are one of the common structural types in regions prone to high seismic risk due to the inherent earthquake resistance of the buildings and ease of construction. Despite their good performance during earthquakes and the abundance of such structures scattered worldwide, current seismic codes and design provisions provide insufficient guidelines for their seismic design. As a compensatory measure, a series of modal and nonlinear dynamic analyses are conducted by emphasizing the characteristic dynamic behavior of tunnel-form buildings under low-intensity seismic actions. This research performs a detailed 3-D finite element analysis on a 16-story tunnel-form reinforced concrete structure using the advanced FE program ABAQUS CAE. Internal seismic damage in the critical region was presented.

Keywords: Tunnel-form, low intensity seismic, ABAQUS, Non-linear analysis

1. Introduction

The tunnel-form concrete structural system is an innovative industrial construction method that streamlines construction management, reduces project timelines, and minimizes financial risks. Unlike conventional frame structures, this system eliminates the need for columns and beams, as the wall and slab elements resist both lateral and gravitational loads. By casting walls and slabs simultaneously, it overcomes common cold joint issues and ensures a uniform three-dimensional performance under seismic loads. As a result, the system is increasingly favored for large-scale construction projects, particularly in seismically active regions. Over the past two decades, numerous studies have explored various aspects of tunnel-form concrete structures, with findings consistently highlighting their high strength and excellent seismic performance. [1-7]

A review of previous research on tunnel-form concrete structures reveals that the behavior of this system under sequential seismic events has not yet been thoroughly explored. Following significant earthquakes, multiple aftershocks, which are typically weaker than the main event, often occur near the same fault that caused the original earthquake. Observations from recent earthquakes, such as the 2010 Chile earthquake, the 2011 Van earthquake in Turkey, and the 2012 Ahar and 2017 Kermanshah earthquakes in Iran, highlight the importance of considering aftershocks during the design process to enhance seismic reliability, particularly in regions with high seismic risk. This issue has gained increasing attention in the fields of structural and earthquake engineering, especially over the past two decades. [8].

Designing high-rise reinforced concrete (RC) buildings presents a significant challenge, particularly in ensuring sufficient lateral resistance to seismic forces. The Kurdistan Region is frequently affected by seismic activity, with vibrations often felt across vast areas. For example, the 7.3-magnitude earthquake on November 12, 2017, near Sarpol-e Zahab along the Iran-Iraq border, resulted in considerable ground shaking throughout the region. Given this seismic context, performing numerical analyses is crucial to accurately assess the behavior of high-rise tunnel-form buildings during earthquakes, helping to mitigate potential risks.

Due to the region's seismic characteristics, high-rise tunnel-form buildings need to be evaluated for their response to minor seismic actions, especially considering the influence of aftershocks and low-intensity seismic events. The objective of this study is to investigate how these buildings, designed for rapid construction and cost-efficiency, perform under low-intensity seismic forces. To achieve this, a 16-story tunnel-form building was analyzed using the finite element program Abaqus through non-linear dynamic analysis. This method allows for a detailed evaluation of the building's response to seismic forces.

2. Structural model

In this study, a 16-story reinforced concrete tunnel-form building is modeled using the three-dimensional finite element software ABAQUS [9] for the analysis. The floor system consists of a flat slab with a thickness of 160 mm, while the shear walls are 200 mm thick. The floor height is 3.0 meters. The building is initially subjected to gravity loads and a uniformly distributed live load of 500 kg/m². Figure 1 illustrates the geometric properties of the building's plan layout.

Figure 1. Details of the Structural Model

3. Finite Element and Non-Linear Numerical Analysis for RC Structures

The ABAQUS program [9] is a powerful, intuitive, finite element program. The program is completely modular, allowing the user to acquire and load only the modules that are needed. The input data for the program include nodal points, type of element, loading condition, material properties, dimensioning of the geometry of the structure, the restraints of nodes, the required type of analysis and the termination criteria.

In order to obtain an accurate analysis, proper material models were needed. To be able to understand the mechanical behavior to final failure, it was important that this non-linear behavior could be simulated in the finite element analyses. The nonlinearities of the concrete in compression and the steel were accounted for with plasticity models. Three major effects cause the non-linear response of reinforced concrete, namely (Crushing of concrete in compression, Cracking of concrete in tension, and Yielding of reinforcement). The steel elements were provided with an isotropic multi-linear elasto-plastic material model.

In this study, ABAQUS/dynamic implicit was adopted to simulate the process of progressive collapse. C3D8R solid elements were used to simulate the concrete components: the beam, column, and slab, and the steel reinforcement embedded inside the concrete member using the 'embedded region' constraints, and is modeled by truss element T3D2. For the sake of reducing the computational time and because, in this study, the overall behaviour of the building is assessed, a large mesh size is used. The density, Young's modulus, and Poisson's ratio of the concrete used in this finite element modelling were 2400 kg/m3, 32 MPa, and 0.2, respectively, and the corresponding properties of steel were 7800 kg/m3, 195 GPa, and 0.3, respectively. The concrete damaged plasticity model was adopted for the concrete constitutive model. The Concrete Damage Plasticity (CDP) model is based on work proposed by [10, 11].

To characterize the constitutive behaviour of concrete, four different laws need to be defined: compressive and tensile behaviour of concrete, damage function, yield function, and flow rule. The behaviour of concrete in uniaxial compression and tension, considered in the CDP model, is shown in Figure 2. In case of compression, a linear-elastic response is considered till the initial yield point, σ_{co}. Whereas, in tension, a linear stress-strain relationship is considered up to the ultimate stress, σ_{to}. In the post-peak region (plastic region), the unloading curve shows a degraded stiffness both in compression and tension. This degradation is due to the damage to the material. The model introduces two damage variables, d_c and d_t, to define this degradation. The range of these variables is 0 to 1, depending on the level of damage. Zero represents "undamaged" and one represents " fully damaged". E_o is the initial (undamaged) modulus of elasticity of concrete. ε_c^{in} and $\varepsilon_c^{pl}$are compressive inelastic and plastic strain, and ε_t^{ck} and ε_t^{pl} are tensile cracking and plastic strain, respectively. The stress-strain behaviour both in compression and tension is considered as follows [9]

$$\sigma_t = (1 - d_t)E_o\left(\varepsilon_t - \varepsilon_t^{pl}\right) \tag{1}$$

$$\sigma_c = (1 - d_c)E_o\left(\varepsilon_c - \varepsilon_c^{pl}\right) \tag{2}$$

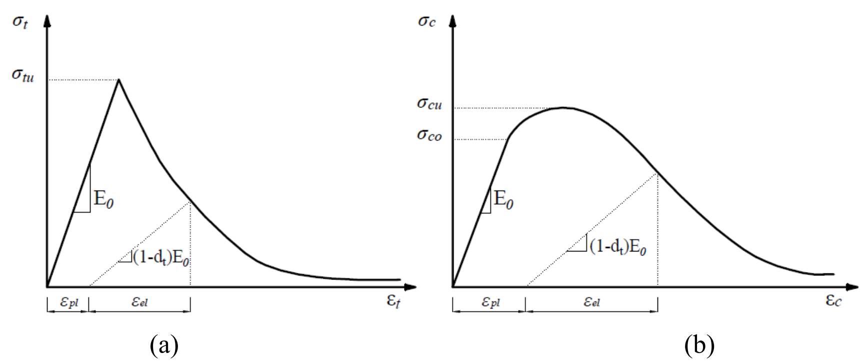

Figure 2. Concrete Damage Plasticity material: uniaxial response in compression (a) and tension (b) [Redrawn based on ABAQUS [9]]

Tensile cracking and compressive crushing are the two failure mechanisms considered in the

CDP model. In these mechanisms, the failure surfaces are controlled by the tensile and compressive plastic strains (ε_c^{pl} and ε_t^{pl}). These strains are automatically calculated in the software from the cracking strain and inelastic strain (ε_t^{ck} and ε_c^{in}) following the equations.

$$\varepsilon_t^{pl} = \varepsilon_t^{ck} - \frac{d_t}{1 - d_t}\frac{\sigma_t}{E_o} \tag{3}$$

$$\varepsilon_c^{pl} = \varepsilon_c^{in} - \frac{d_c}{1 - d_c}\frac{\sigma_c}{E_o} \tag{4}$$

Two model inputs are needed to define the yield function in the model; the ratio of biaxial to uniaxial compressive stress (σ_{bo}/σ_{co}default value is 1.16) and the ratio of the tensile and compressive second invariant (K_c, default value is 2/3). K_c controls the shape of failure surface in the deviatoric plane A non-associated plastic flow is presumed by CDP model where the Drucker-Prager hyperbolic function is used as flow potential. The function is as follows

$$G = \sqrt{(\in \sigma_t tan\psi)^2 + q^2} - ptan\psi \tag{5}$$

Where, ψ = dilation angle which is measured in the $p - q$ plane at high confining pressure; $\in$ = eccentricity. The default value of eccentricity is 0.1.

The CDP model requires the values of and K_c to define the yield function as well as ψ and $\in$ to define the flow rule. This model uses the default values of σ_{bo}/σ_{co}, K_c, and $\in$ as 1.16, 2/3, and 0.1, respectively. A dilation angle of 30^o is considered in this study. A special parameter, the viscosity parameter, needs to be defined in the model that controls the convergence of the model.

Two different parameters, modulus of elasticity (E_c) and Poisson's ratio, are to be input to define the elastic property of the material. In this study, 0.2 is chosen as the Poisson's ratio. The E_c was calculated by the equation given by ACI 318 as follows

$$E_c = 57000\sqrt{f_c'}\,psi \tag{6}$$

To define the stress-strain relationship in compression, the model proposed by Popovics [12] was used in this study. The relationship is shown in the following equation,

$$f_c = f_c'\frac{\varepsilon_c}{\varepsilon_{co}}\frac{n}{n - 1 + (\varepsilon_c/\varepsilon_{co})^n} \tag{7}$$

Where f_c', ε_{co} are the compressive strength and strain corresponding to the maximum stress, respectively. The *n* is defined by,

$$n = 0.4 \cdot 10^{-3} f_c(psi) + 1.0 \tag{8}$$

Whereas, the tensile stress–strain relationship of concrete was in accordance with (Shakib and Morshed [13]), can be obtained by the following:

$$\sigma = F_t\left(\frac{\varepsilon_t}{\varepsilon}\right)^{0.7} \tag{9}$$

$$\varepsilon_t = \frac{F_t}{\varepsilon_c} \tag{10}$$

Eigen-frequency analyses were conducted on the 3D FE models in order to obtain a preliminary insight into the dynamic behavior of the buildings under study, identifying the main vibration modes, the corresponding periods, and the participating mass ratios.

The seismic response of the building was then investigated through non-linear dynamic analysis; the ground motions were applied to the building in the horizontal directions X-axis and Z-axis. With the aim of simulating the seismic response of the building under low-intensity seismic loads, the PGA value was used by scaling the real accelerograms (registered on November 12 during the 2017 Sarpol-e Zahab (M_w = 7.3), Iran-Iraq border earthquake) through the software code

SeismoMatch [14]. Fig. 3 shows the horizontal component of the accelerogram. The duration of the real frequency is equal to 99.44s. In this study, we chose 25 seconds of high intensity because of the high computational demand required by the analyses. The PGA of 0.05g was used in the non-linear dynamic analyses. The non-linear dynamic analyses with PGA=0.05g aim at simulating the seismic response of the building to earthquakes of low intensity magnitudes and provide useful information about the seismic response and damage distribution of the building for small PGA values.

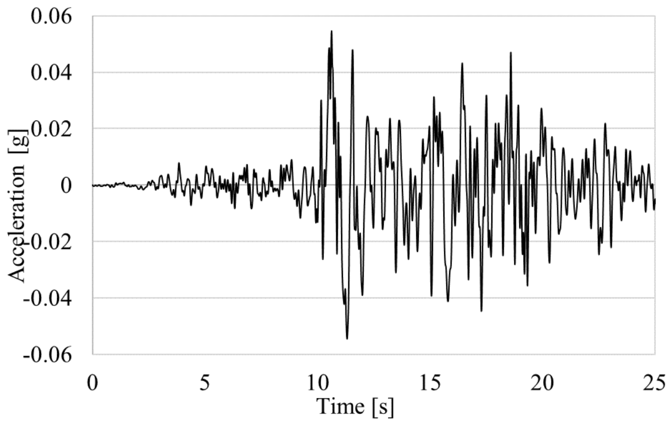

Figure 3. Scaled accelerogram (Horizontal component of the Ezgeleh (Sarpol-e Zahab), Iran-Iraq border earthquake, 12 November 2017) used in the non-linear dynamic analyses

4. Results and discussions

The linear perturbation analysis is performed to calculate the natural periods of the building. Using the Lanczos algorithm, the first 100 natural modes are calculated. The distribution of the first hundred modes in the two orthogonal directions is presented in Fig. 4. Moreover, Fig. 5 shows the deformed shapes and the corresponding periods of the main vibration modes with a participating mass ratio (PMR) larger than about 5% for the building.

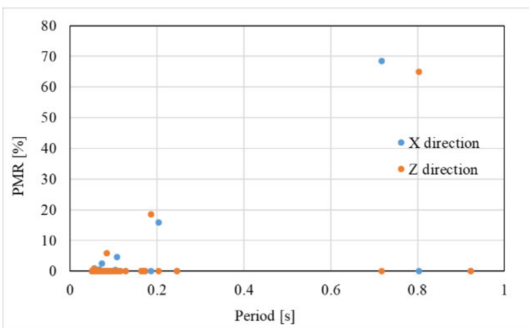

Figure 4. Distribution of the first three hundred modes in the horizontal (X and Z) directions

The first two main modes are Mode 2 (T=0.8 s), involving the whole building with PMR equal to 65% in the Z direction, and Mode 3 (T=0.716 s), involving the whole building with PMR equal to 68.5% in the X direction. The most relevant modes are Mode 6 (T=0.096 s) with the largest PMR (76.4%) in the y direction. The first hundred modes correspond to a total PMR of 94.25% in the X direction, 91% in the Y direction, and 83.12% in the Z direction.

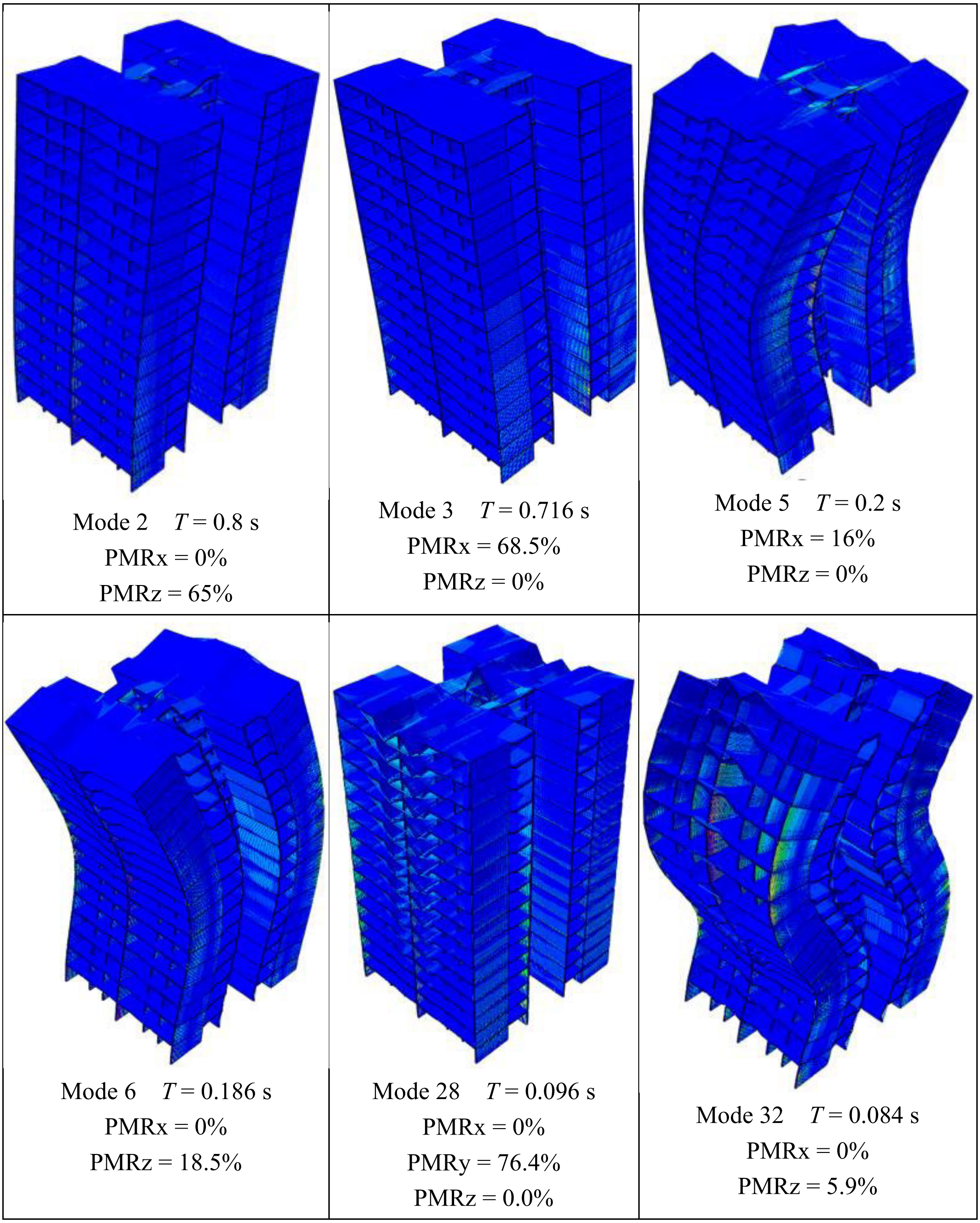

Figure 5. Deformed shapes and corresponding periods of the main vibration modes with indication of the participating mass ratios

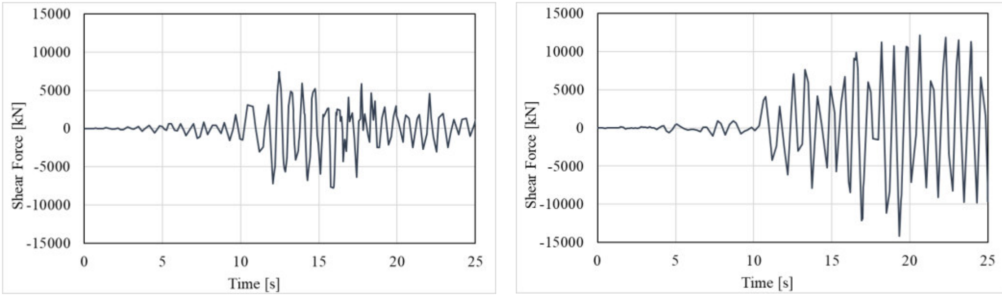

X- Direction *Z- Direction*

Figure 6. Time histories of base shear force for the earthquakes

Time histories of base shear force obtained for both X and Z-Directions are given in Fig. 6. Von-Mises Stress distribution occurred under the earthquake ground motions in X and Z-Directions are shown in Figs. 7 and 8, respectively.

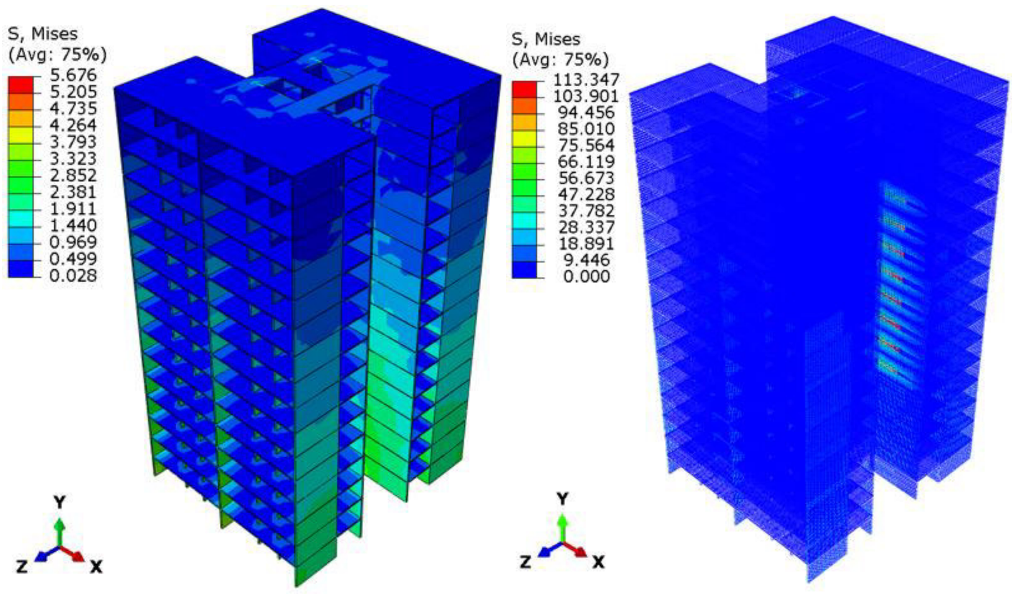

Concrete *Reinforcement*

Figure 7. Von-Mises Stress distribution in the X-Direction

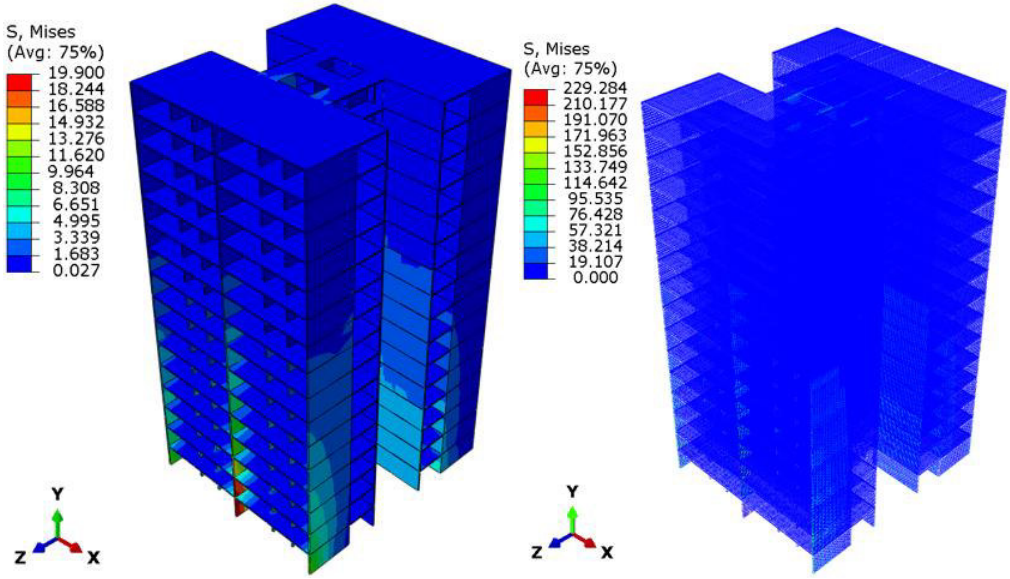

Concrete *Reinforcement*

Figure 8. Von-Mises Stress distribution in the Z-Direction

Under seismic action in the Z-Direction (stiff side), it can be said that the maximum stress in the concrete and steel reinforcement can be found at the base of the building, the 1st floor, and the 2nd floor levels. The 1st and 2nd floor level reinforcement von-Mises stress distribution and concrete tensile damage are illustrated in Fig. 9. Tensile strain is one of the main reasons causing buckling to the reinforcing bars in RC columns, especially in this situation, as the concrete failed under tensile stress.

The building under seismic action in the X-Direction (flexible side) has a stress distribution in the middle stores. The middle stores reinforcement von-Mises stress distribution and concrete tensile damage, illustrated in Fig. 10.

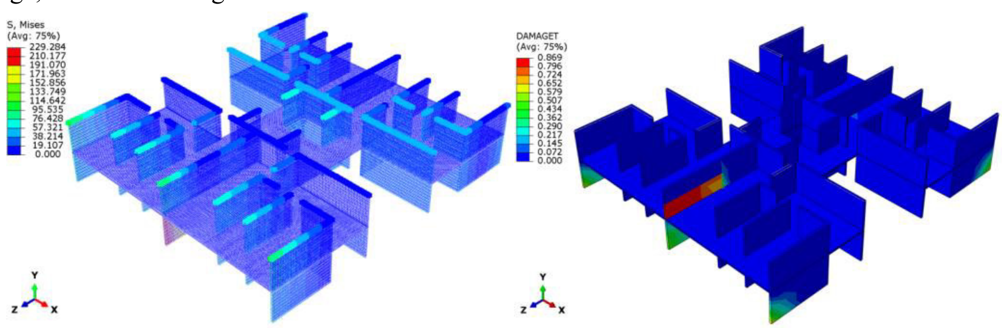

Figure 9. 1st and 2nd floor level (a) Reinforcement Von-Mises Stress distribution in the Z-Direction (b) Concrete tensile damage in the Z-Direction

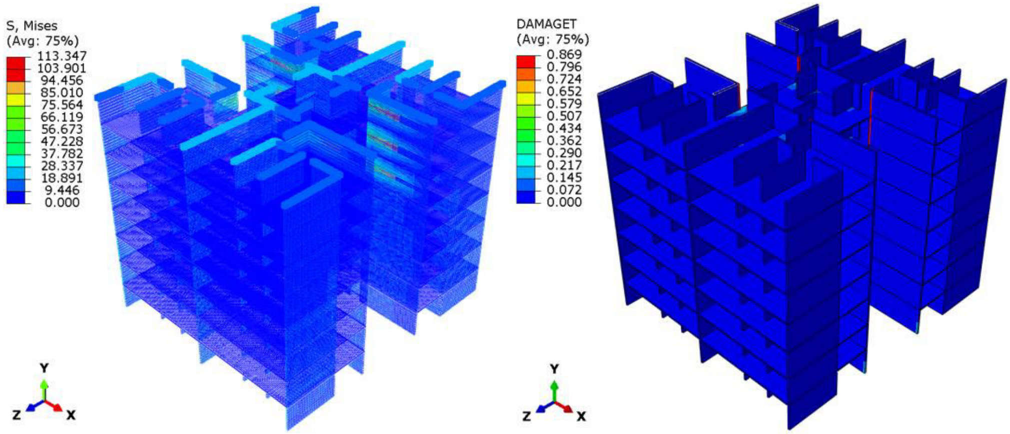

Figure 10. Middle stores (a) Reinforcement Von-Mises Stress distribution in the X-Direction (b) Concrete tensile damage in the X-Direction

5. Conclusion

The aim of this study was to investigate the behavior of tunnel-form concrete structures under low-intensity seismic loads. To achieve this, a scaled version of the main-shock seismic frequency was applied to represent low-intensity seismic conditions. A prototype 16-story tunnel-form building was analyzed using non-linear dynamic analysis. The numerical procedure presented in this study focuses on identifying the most critical regions along the height of the building. The findings demonstrated that conducting structural analysis using advanced finite element modeling and non-linear dynamic analysis is crucial for understanding the overall structural behavior and pinpointing the vulnerable areas of tunnel-form buildings subjected to low-intensity seismic actions.

6. References

[1] Balkaya, C. and Kalkan, E., 2004. Seismic vulnerability, behavior and design of tunnel form building structures. *Engineering Structures*, *26*(14), pp.2081-2099.

[2] Kalkan, E. and Yüksel, S.B., 2008. Pros and cons of multistory RC tunnel-form (box-type) buildings. *The Structural Design of Tall and Special Buildings*, *17*(3), pp.601-617.

[3] Yüksel, S.B., 2008. Slit-connected coupling beams for tunnel-form building structures conditions. *The Structural Design of Tall and Special Buildings*, *13*(3), pp.579-600.

[4] Behesthi Aval, S.B., Mohsenian, V. and Sadegh Kouhestani, H., 2018. Seismic performance-based assessment of tunnel form building subjected to near-and far-fault ground motions. *Asian Journal of Civil Engineering*, *19*, pp.79-92.

[5] Mohsenian, V. and Mortezaei, A., 2018. Seismic reliability evaluation of tunnel form (box-type) RC structures under accidental torsion. *Structural concrete*, *19*(6), pp.1927-1938.

[6] Mohsenian, V., Rostamkalaee, S. and Moghadam, A., 2018, June. Seismic reliability of tunnel form concrete buildings subjected to accidental torsion: a case study. In *16th European Conference on Earthquake Engineering, Thessaloniki, Greece*.

[7] Mortezaei, A. and Mohsenian, V., 2022. Reliability-based seismic assessment of multi-story box system buildings under the accidental torsion. *Journal of Earthquake Engineering*, *26*(2), pp.674-697.

[8] Mohsenian, V., Gharaei-Moghaddam, N. and Hajirasouliha, I., 2021. Seismic performance assessment of tunnel form concrete structures under earthquake sequences using endurance time analysis. *Journal of Building Engineering*, *40*, p.102327.

[9] ABAQUS, online documentation. SIMULIA Inc.; 2018.

[10] Lubliner, J., Oliver, J., Oller, S. and Oñate, E., 1989. A plastic-damage model for concrete. International Journal of solids and structures, 25(3), pp.299-326.

[11] Lee, J. and Fenves, G.L., 1998. Plastic-damage model for cyclic loading of concrete structures. Journal of engineering mechanics, 124(8), pp.892-900

[12] Popovics, S., 1973. A numerical approach to the complete stress-strain curve of concrete. *Cement and concrete research*, *3*(5), pp.583-599.

[13] Shakib, S. and Morshed, A.Z., 2021. Modeling of cover concrete cracking due to uniform corrosion of reinforcement. *Journal of Engineering Science*, pp.43-49.

[14] SeismoSoft. (2021). SeismoMatch - A computer program for spectrum matching of accelerograms.